Electronic Supplementary Information

Phenoxazinone synthase-like catalytic activity of novel mono- and tetranuclear copper(II) complexes with 2-benzylaminoethanol

*Oksana V. Nesterova,[a] Olena Bondarenko,[a] Armando J.L. Pombeiro[a] and Dmytro S. Nesterov[*a,b]*

[a] *Centro de Química Estrutural, Instituto Superior Técnico, Universidade de Lisboa, Av. Rovisco Pais, 1049-001 Lisboa, Portugal;*

[b] *Peoples' Friendship University of Russia (RUDN University), 6 Miklukho-Maklaya st., Moscow 117198, Russia.*

E-mail: dmytro.nesterov@tecnico.ulisboa.pt

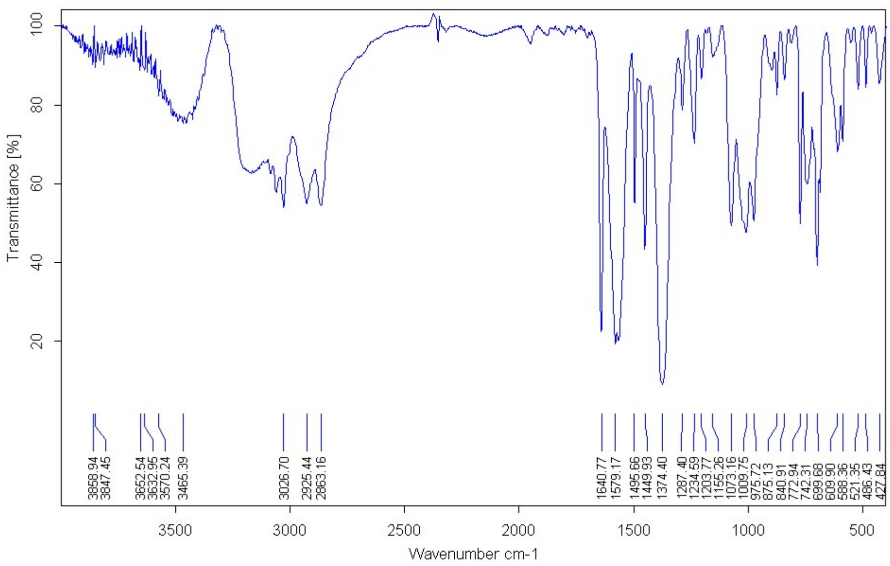

Figure S1. IR spectrum of **1**.

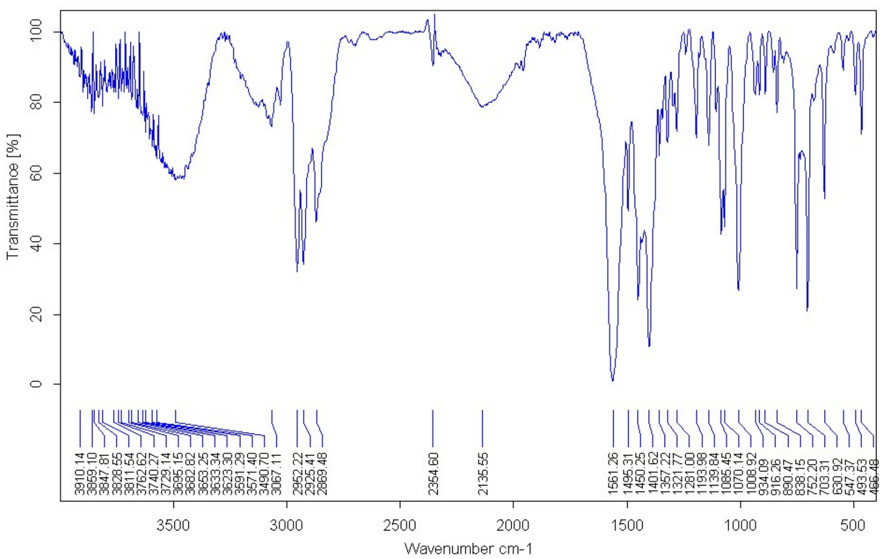

Figure S2. IR spectrum of **2**.

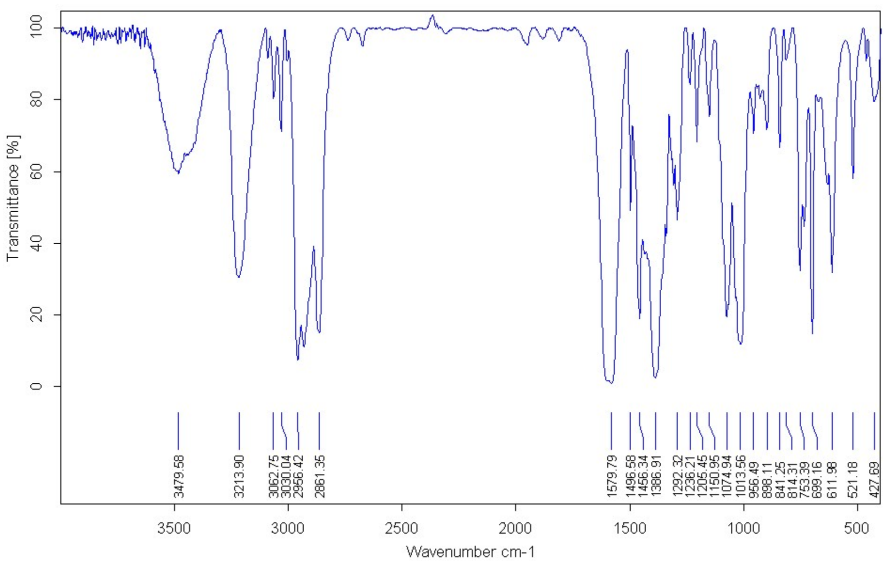

Figure S3. IR spectrum of **3**.

Table S1. Selected geometrical parameters (distances/Å and angles/°) for **1** and **2**.

	1	**2**
Cu1–O1	2.3956(15)	2.411(4)
Cu1–O2	2.0021(12)	1.987(4)
Cu1–N1	2.0275(13)	2.021(4)
O1–Cu1–O1[a]	180	180
O1–Cu1–O2	92.51(6)	86.37(14)
O1–Cu1–O2[a]	87.49(6)	93.63(14)
O1[a]–Cu1–O2[a]	92.51(6)	86.37(14)
O1–Cu1–N1	79.68(5)	79.18(15)
O1–Cu1–N1[a]	100.32(5)	100.82(15)
O2–Cu1–O1[a]	87.49(6)	93.63(14)
O2–Cu1–O2[a]	180	180
O2–Cu1–N1	86.86(6)	92.57(17)
O2–Cu1–N1[a]	93.14(6)	87.43(17)
N1–Cu1–O1[a]	100.32(5)	100.82(15)
N1–Cu1–O2[a]	93.14(6)	87.43(17)
N1–Cu1–N1[a]	180	180
N1[a]–Cu1–O1[a]	79.68(5)	79.18(15)
N1[a]–Cu1–O2[a]	86.86(6)	92.57(17)

Symmetry code: [a] 1–x, 1–y, 1–z.

Table S2. Selected geometrical parameters (separations and distances/Å, and angles/°) for **3**.

Cu1···Cu2	2.8897(10)	Cu5···Cu6	2.9050(11)
Cu1···Cu4	3.3793(11)	Cu5···Cu8	3.3133(10)
Cu1···Cu3	3.4323(11)	Cu5···Cu7	3.4616(10)
Cu2···Cu4	3.3713(11)	Cu6···Cu7	3.3516(11)
Cu2···Cu3	3.3787(11)	Cu6···Cu8	3.4474(11)
Cu3···Cu4	2.8971(11)	Cu7···Cu8	2.8804(11)
Cu1–O1	1.963(3)	Cu5–O13	1.950(3)
Cu1–O2	1.928(4)	Cu5–O14	1.919(3)
Cu1–O4	1.976(3)	Cu5–O16	1.997(3)
Cu1–O10	2.455(3)	Cu5–O19	2.402(3)
Cu1–N1	2.030(4)	Cu5–N5	2.032(4)
Cu2–O1	1.952(3)	Cu6–O13	1.970(3)
Cu2–O4	1.980(3)	Cu6–O16	1.960(3)
Cu2–O5	1.928(4)	Cu6–O17	1.943(3)
Cu2–O7	2.420(3)	Cu6–O22	2.417(3)
Cu2–N2	2.018(4)	Cu6–N6	2.014(4)
Cu3–O1	2.445(3)	Cu7–O16	2.461(3)
Cu3–O7	1.970(3)	Cu7–O19	1.978(3)
Cu3–O8	1.927(4)	Cu7–O20	1.926(3)
Cu3–O10	1.975(3)	Cu7–O22	1.961(3)
Cu3–N3	2.024(4)	Cu7–N7	2.010(4)
Cu4–O4	2.419(3)	Cu8–O13	2.453(3)
Cu4–O7	1.985(3)	Cu8–O19	1.953(3)
Cu4–O10	1.964(3)	Cu8–O22	1.971(3)
Cu4–O11	1.925(4)	Cu8–O23	1.941(3)
Cu4–N4	2.024(4)	Cu8–N8	2.001(4)
O1–Cu1–O2	177.11(16)	O13–Cu5–O14	177.87(15)
O1–Cu1–O4	83.15(12)	O13–Cu5–O16	82.73(12)
O1–Cu1–O10	79.56(11)	O13–Cu5–O19	82.05(11)
O1–Cu1–N1	84.72(15)	O13–Cu5–N5	83.90(14)
O2–Cu1–O4	94.47(15)	O14–Cu5–O16	95.27(14)
O2–Cu1–O10	102.82(13)	O14–Cu5–O19	98.28(12)
O2–Cu1–N1	97.38(16)	O14–Cu5–N5	97.93(16)
O4–Cu1–O10	79.56(11)	O16–Cu5–O19	77.85(11)
O4–Cu1–N1	165.23(15)	O16–Cu5–N5	162.74(14)
O10–Cu1–N1	106.20(13)	O19–Cu5–N5	111.01(13)
O1–Cu2–O4	83.32(12)	O13–Cu6–O16	83.19(12)
O1–Cu2–O5	94.66(16)	O13–Cu6–O17	94.11(14)
O1–Cu2–O7	80.18(11)	O13–Cu6–O22	77.98(11)
O1–Cu2–N2	165.34(16)	O13–Cu6–N6	164.82(15)
O4–Cu2–O5	176.40(16)	O16–Cu6–O17	176.59(15)
O4–Cu2–O7	80.42(11)	O16–Cu6–O22	81.14(11)
O4–Cu2–N2	84.90(15)	O16–Cu6–N6	84.74(16)
O5–Cu2–O7	102.22(13)	O17–Cu6–O22	100.38(13)
O5–Cu2–N2	96.61(18)	O17–Cu6–N6	97.58(17)
O7–Cu2–N2	106.41(14)	O22–Cu6–N6	109.19(13)
O1–Cu3–O7	79.23(11)	O16–Cu7–O19	76.74(11)
O1–Cu3–O8	100.58(13)	O16–Cu7–O20	103.44(13)
O1–Cu3–O10	78.44(11)	O16–Cu7–O22	79.98(11)
O1–Cu3–N3	106.76(13)	O16–Cu7–N7	105.66(13)
O7–Cu3–O8	178.25(14)	O19–Cu7–O20	177.47(15)
O7–Cu3–O10	83.46(12)	O19–Cu7–O22	82.80(12)
O7–Cu3–N3	84.43(15)	O19–Cu7–N7	85.11(14)

O8–Cu3–O10	94.80(14)	O20–Cu7–O22	94.73(15)
O8–Cu3–N3	97.28(16)	O20–Cu7–N7	97.25(16)
O10–Cu3–N3	165.66(15)	O22–Cu7–N7	165.10(15)
O4–Cu4–O7	80.34(11)	O13–Cu8–O19	80.65(10)
O4–Cu4–O10	80.70(11)	O13–Cu8–O22	77.08(11)
O4–Cu4–O11	98.51(13)	O13–Cu8–O23	103.62(13)
O4–Cu4–N4	107.13(14)	O13–Cu8–N8	104.32(13)
O7–Cu4–O10	83.34(12)	O19–Cu8–O22	83.17(12)
O7–Cu4–O11	95.48(15)	O19–Cu8–O23	92.84(14)
O7–Cu4–N4	164.78(15)	O19–Cu8–N8	166.08(15)
O10–Cu4–O11	178.68(15)	O22–Cu8–O23	175.81(14)
O10–Cu4–N4	84.83(15)	O22–Cu8–N8	85.28(14)
O11–Cu4–N4	96.43(18)	O23–Cu8–N8	98.48(16)

Table S3. Hydrogen bonding distances (Å) and angles (°) for complexes **1–4**.

D–H···A	D–H	H···A	D···A	D–H···A
1				
O1–H1···O3[a]	0.75(3)	1.95(3)	2.680(2)	164(3)
N1–H2···O3[b]	0.79(2)	2.13(2)	2.8322(19)	148(2)
2				
O1–H2···O3[c]	0.92(4)	1.75(4)	2.666(5)	170(4)
N1–H1···O3	0.85(5)	2.18(5)	2.877(6)	139(4)
3				
N1–H1C···O24[d]	0.98	2.25	3.115(6)	146.0
N2–H2C···O21[d]	0.98	2.24	3.097(6)	144.9
N3–H3C···O15	0.98	2.09	2.977(6)	149.6
N4–H4A···O18	0.98	2.10	2.997(6)	150.8
N5–H5B···O9	0.98	2.04	2.951(6)	153.7
N6–H6B···O12	0.98	2.18	3.062(6)	148.6
N7–H7B···O6[e]	0.98	2.17	3.076(6)	152.7
N8–H8B···O3[e]	0.98	2.21	3.083(6)	147.1
4				
O1–H3···N1[f]	0.91(2)	1.87(2)	2.7696(13)	167.7(18)
N1–H2···O1[g]	0.856(17)	2.259(17)	3.0576(13)	155.5(14)

Symmetry codes: [a] –x, 1–y, 1–z; [b] 1–x, 1–y, 1–z; [c] x, y, –1+z; [d] 1+x, y, z; [e] –1+x, y, z; [f] x–1/2, –y+1/2, 1–z; [g] 1–x, –y, 1–z.

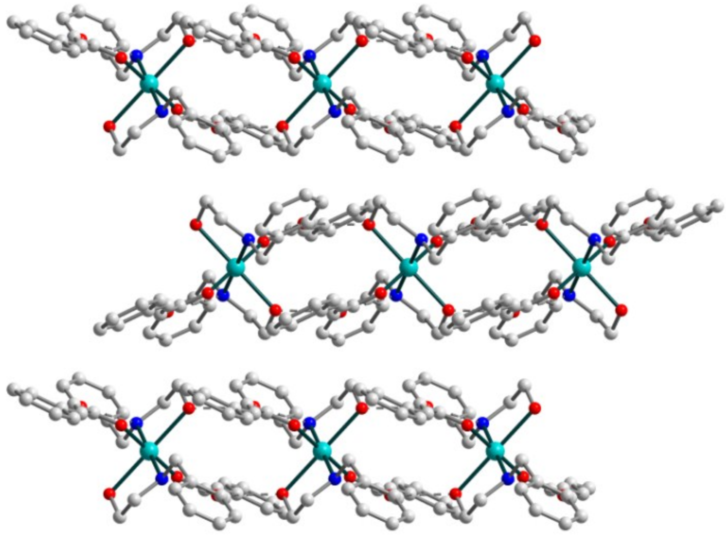

a

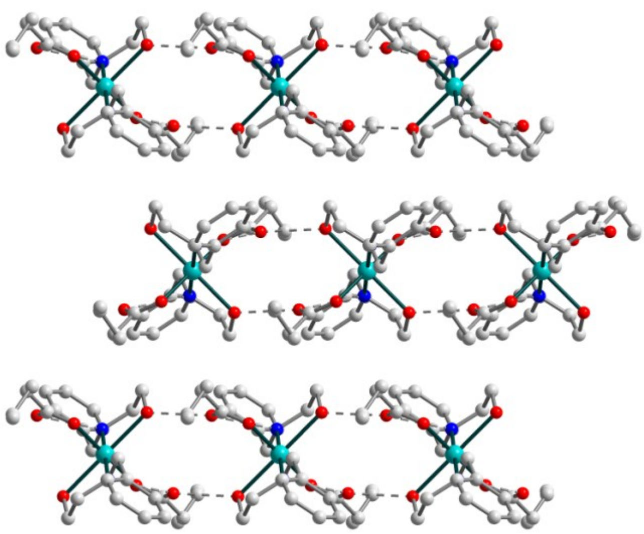

b

Figure S4. The representation of the packing of supramolecular chains in **1** down the *c* axis (*a*) and **2** down the *a* axis (*b*). H atoms are omitted for clarity. Colour scheme: Cu, cyan; O, red; N, blue; C, grey.

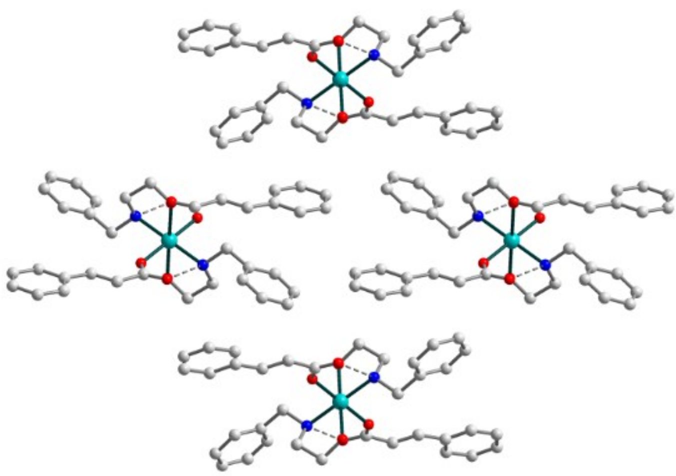

Figure S5. The representation of the packing of supramolecular chains in **1** down the *a* axis. H atoms are omitted for clarity. Colour scheme: Cu, cyan; O, red; N, blue; C, grey.

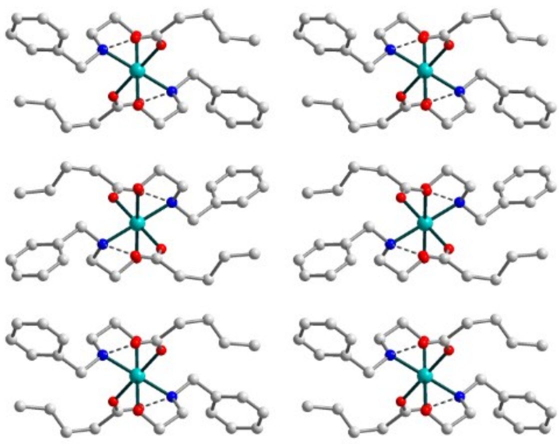

Figure S6. The representation of the packing of supramolecular chains in **2** down the *c*. H atoms are omitted for clarity. Colour scheme: Cu, cyan; O, red; N, blue; C, grey.

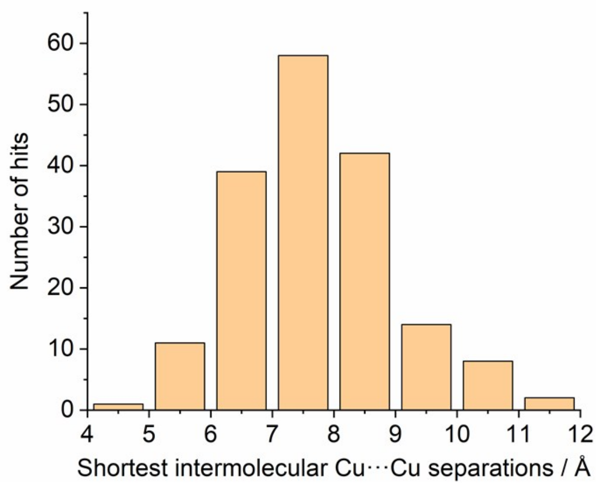

Figure S7. The diagram showing the shortest intermolecular Cu···Cu separations in the crystal structures of Cu_4O_4 molecular complexes, basing on the CSD data.

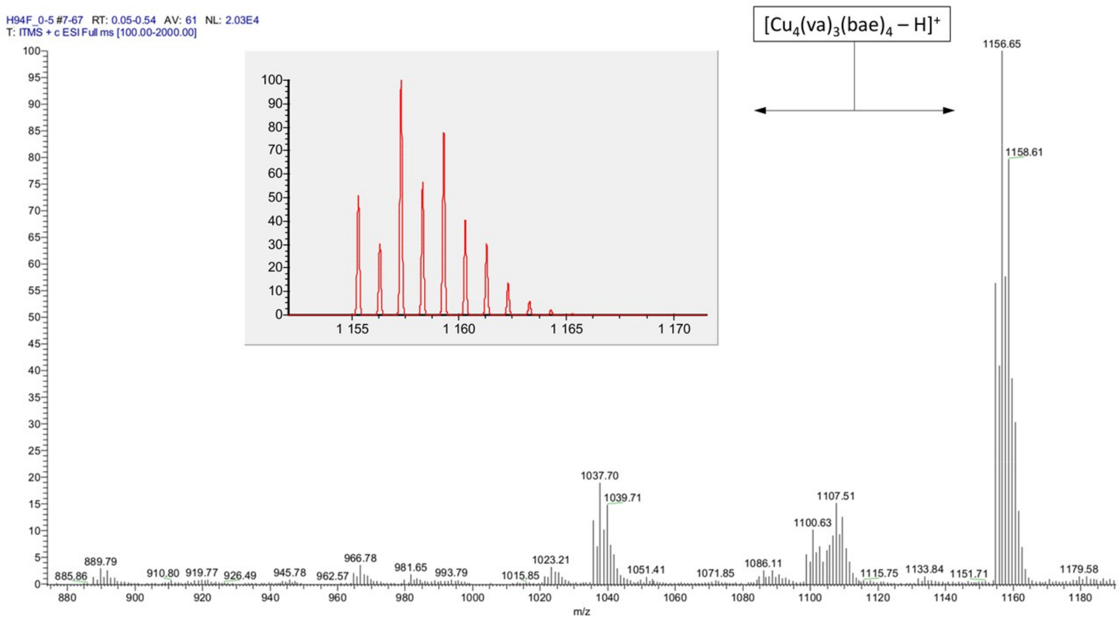

Figure S8. Fragment of the ESI-MS spectrum of **2** showing the experimental and theoretical (inset) MS isotopic patterns for $[Cu_4(va)_3(bae)_4 - H]^+$.

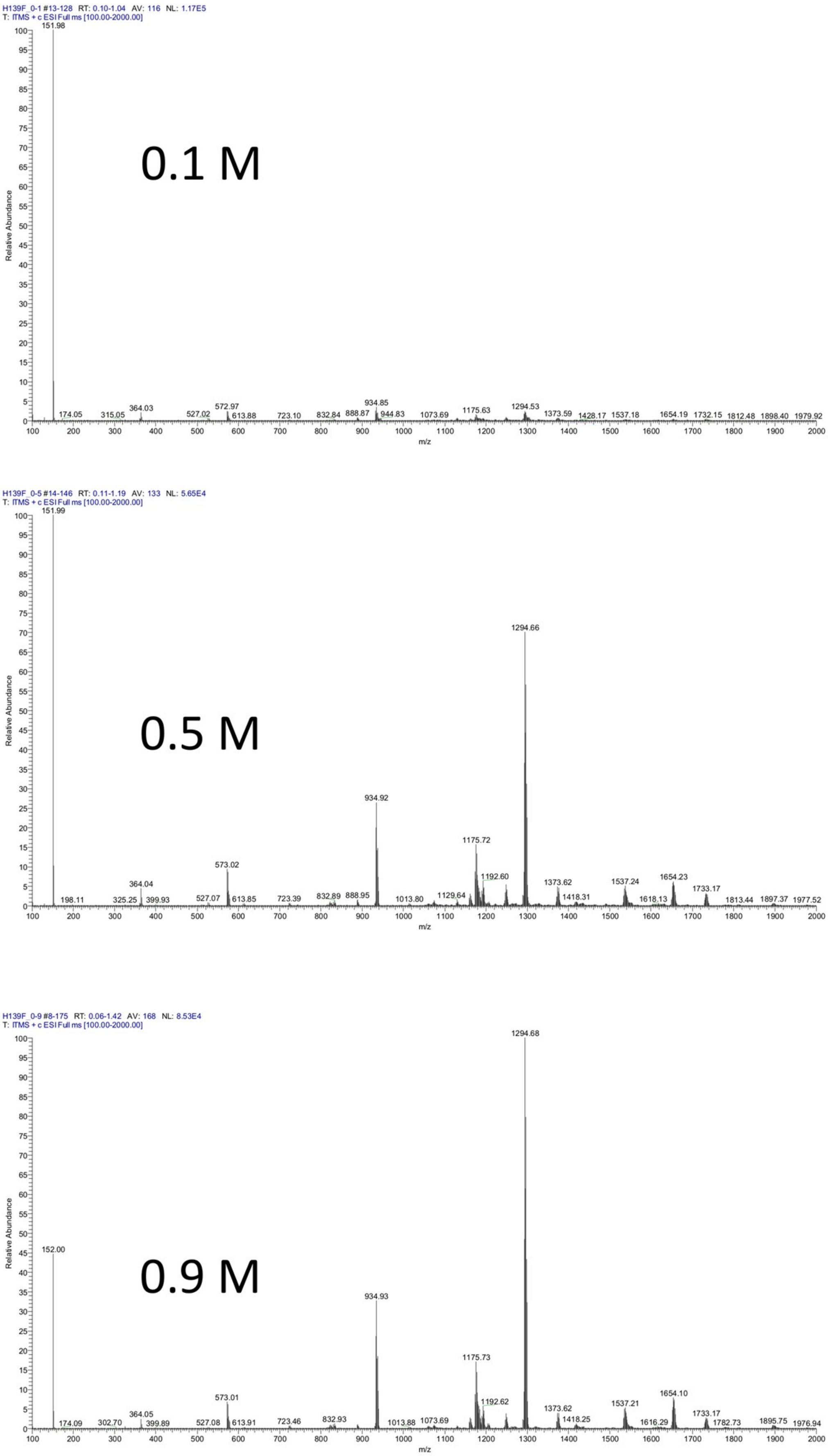

Figure S9. ESI-MS spectra of **1** in methanol depending on the full concentration of copper.

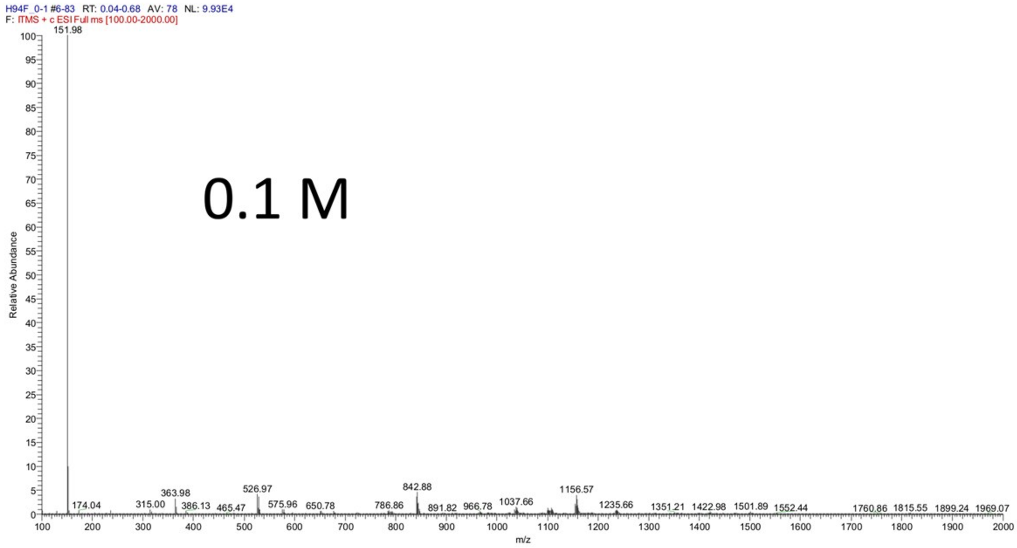

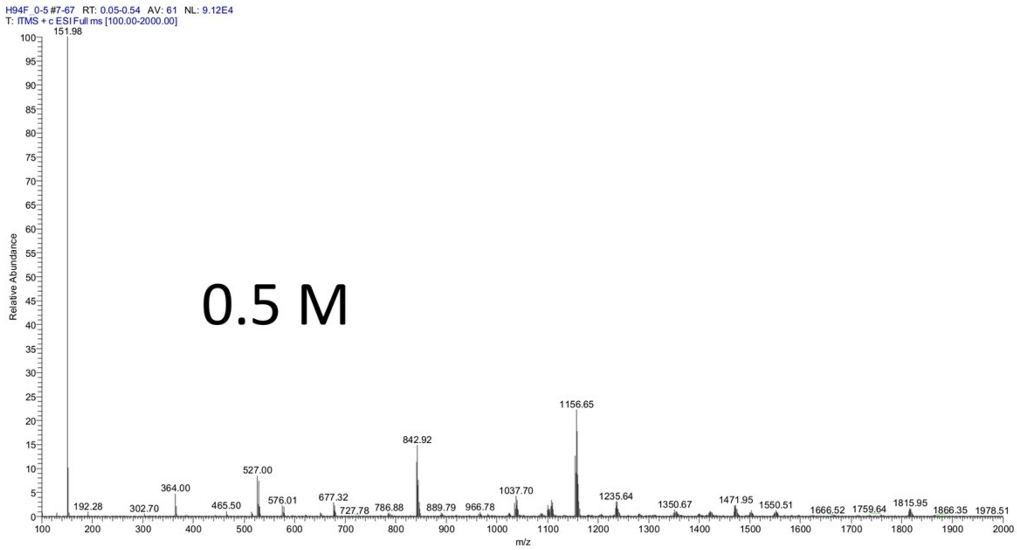

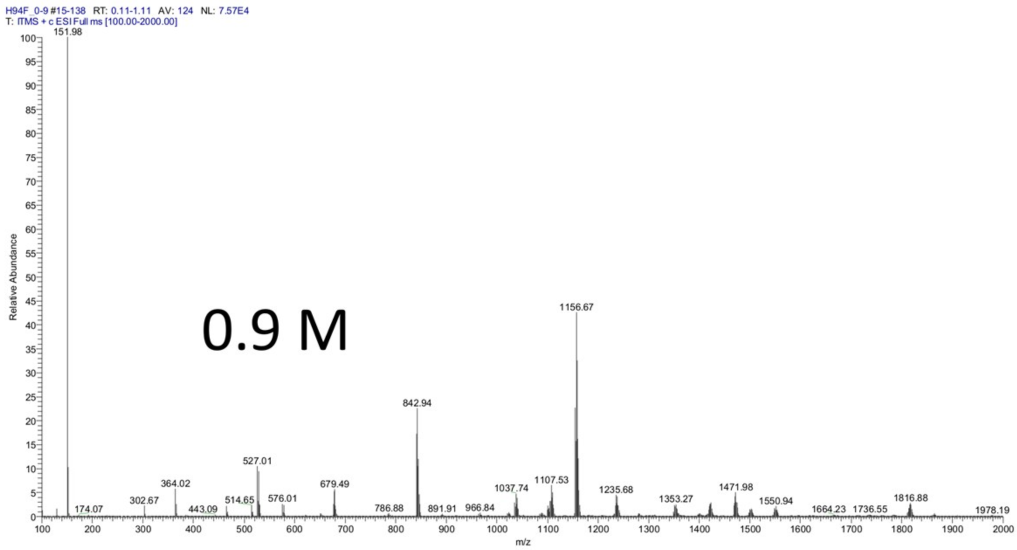

Figure S10. ESI-MS spectra of **2** in methanol depending on the full concentration of copper.

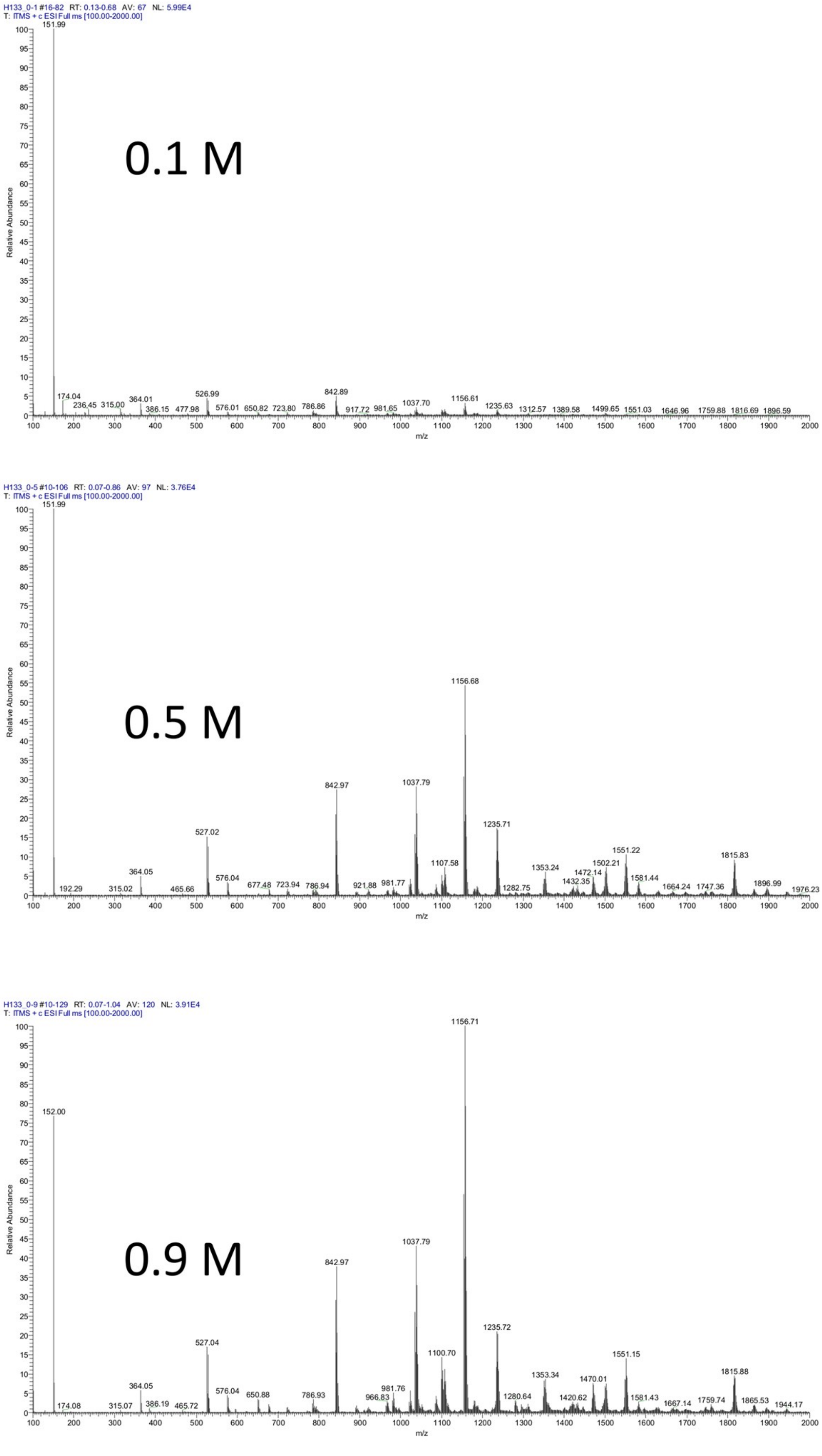

Figure S11. ESI-MS spectra of **3** in methanol depending on the full concentration of copper.

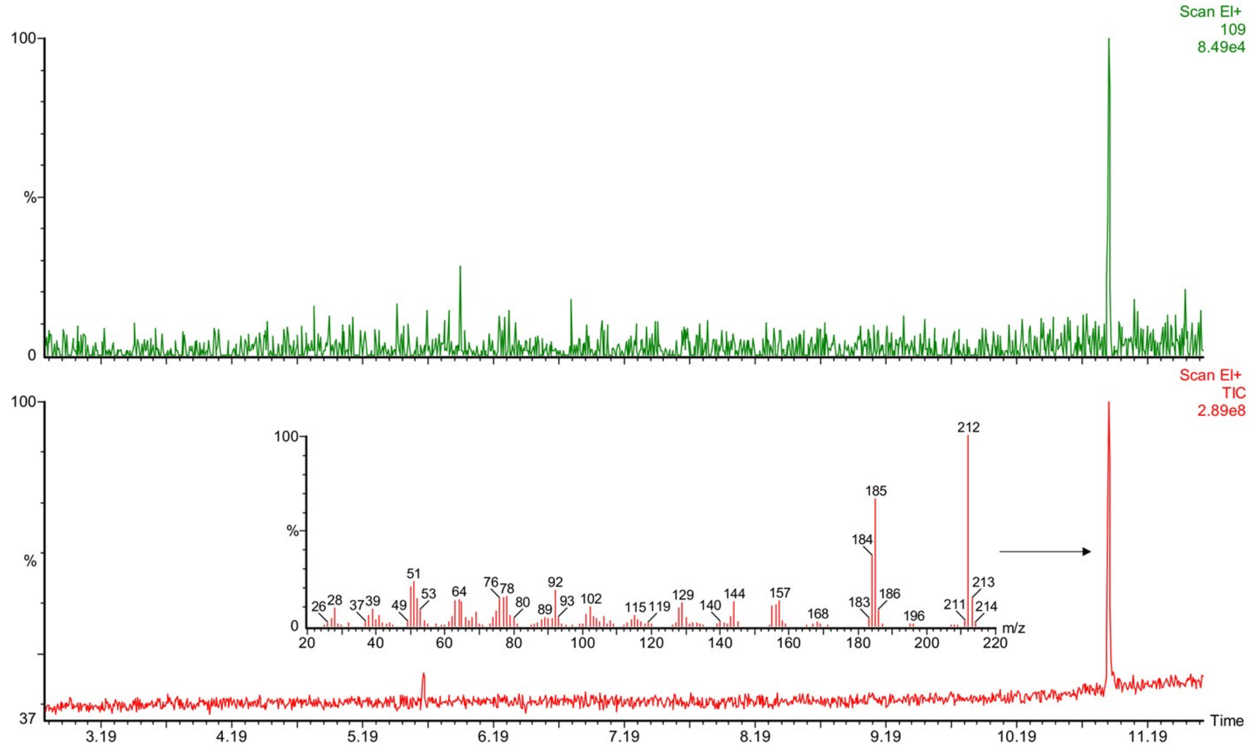

Figure S12. Fragments of the chromatogram (bottom) showing the peak of a phenoxazinone chromophore (at 10.9 min) after 24 h oxidation of OAP catalysed by 2 mM of **2**. The inset shows the respective EI mass spectrum. The top chromatogram shows the intensity of 109 m/z signal, corresponding to a substrate (OAP), indicating the complete conversion of OAP.

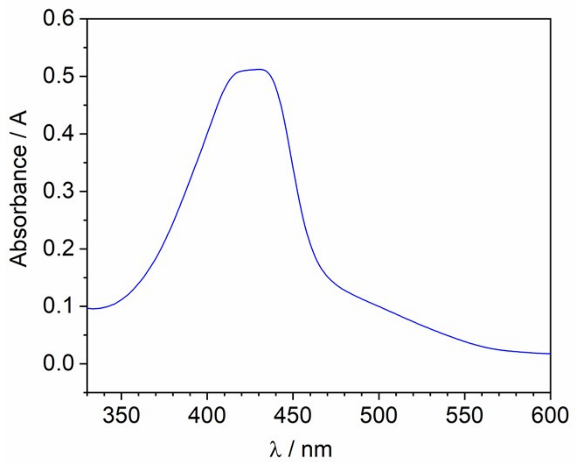

Figure S13. UV-Vis spectrum of the solution obtained after 24 h stirring of 0.01 mM of OAP and 1.1 mM of **3** in methanol, under inert atmosphere. Due to strong absorbance of phenoxazinone chromophore direct measurement of solution spectrum was not possible. Instead, 0.5 mL of reaction mixture was diluted with 4 mL of methanol, the resulting solution was immediately transferred to UV cuvette. Further measurements performed after 5 and 10 min did not show notable changes of absorbance.

Table S4. Initial reaction rates W_0 of the OAP (0.01 M) oxidation with air dioxygen in methanol, catalysed by copper complexes (1 mM of total copper concentration).

Catalyst	W_0, M s^{-1}	Reference
1	1.3×10^{-7}	this work
2	7.0×10^{-8}	this work
3	4.0×10^{-8}	this work
$[Cu^{II}_8O(t\text{bdea})_6(H_2O)_2](BF_4)_2\cdot 3CH_3OH$[a]	7.7×10^{-9}	[30]
$[Cu^{II}_8O(t\text{bdea})_5(Ht\text{bdea})Cl_2][Cu^{I}Cl_2]\cdot 2H_2O$	2.2×10^{-8}	[31]
$[Cu^{I}(CH_3CN)_2](PF_6)$	8.6×10^{-8}	this work
$Cu(OAc)_2$	3.7×10^{-8}	this work
$CuCl_2$[b]	8.4×10^{-8}	this work
$Cu(NO_3)_2$	3.5×10^{-7}	this work
$Cu(NO_3)$ / bipy[c]	4.7×10^{-8}	this work
3 / bipy	1.3×10^{-7}	this work

[a] H_2tbdea = *N*-*tert*-butyldiethanolamine; [b] 0.5 mM of the catalyst was used; [c] bipy = 2,2’-bipyridine (1 mM).

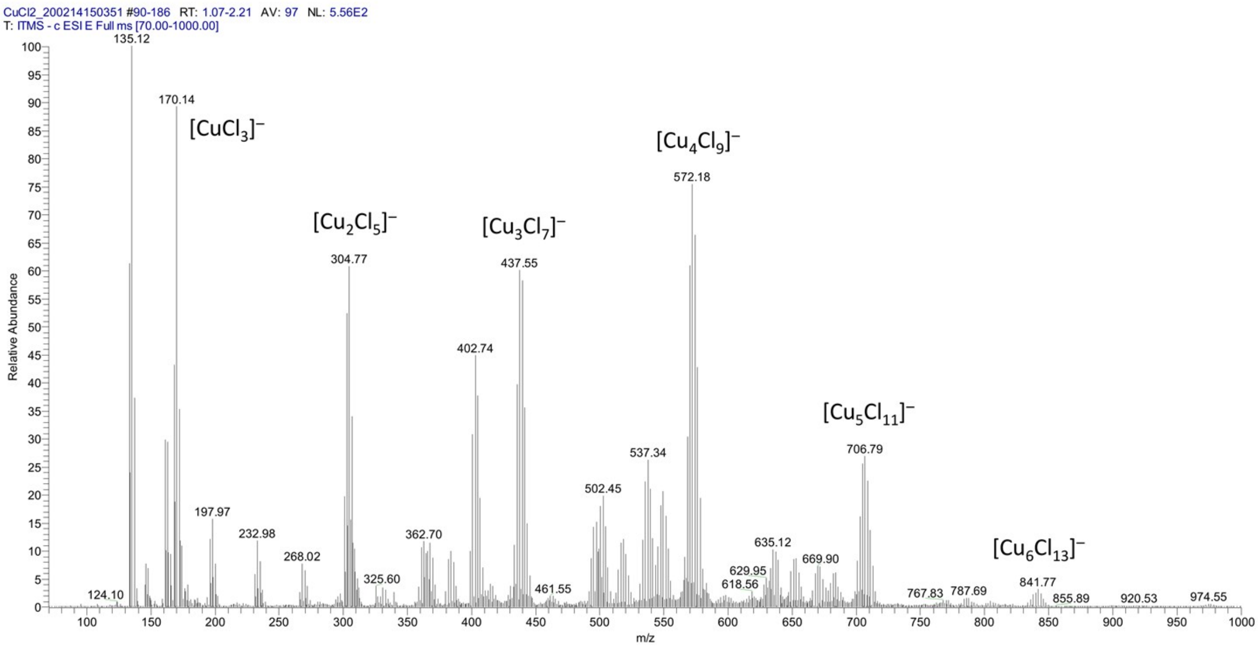

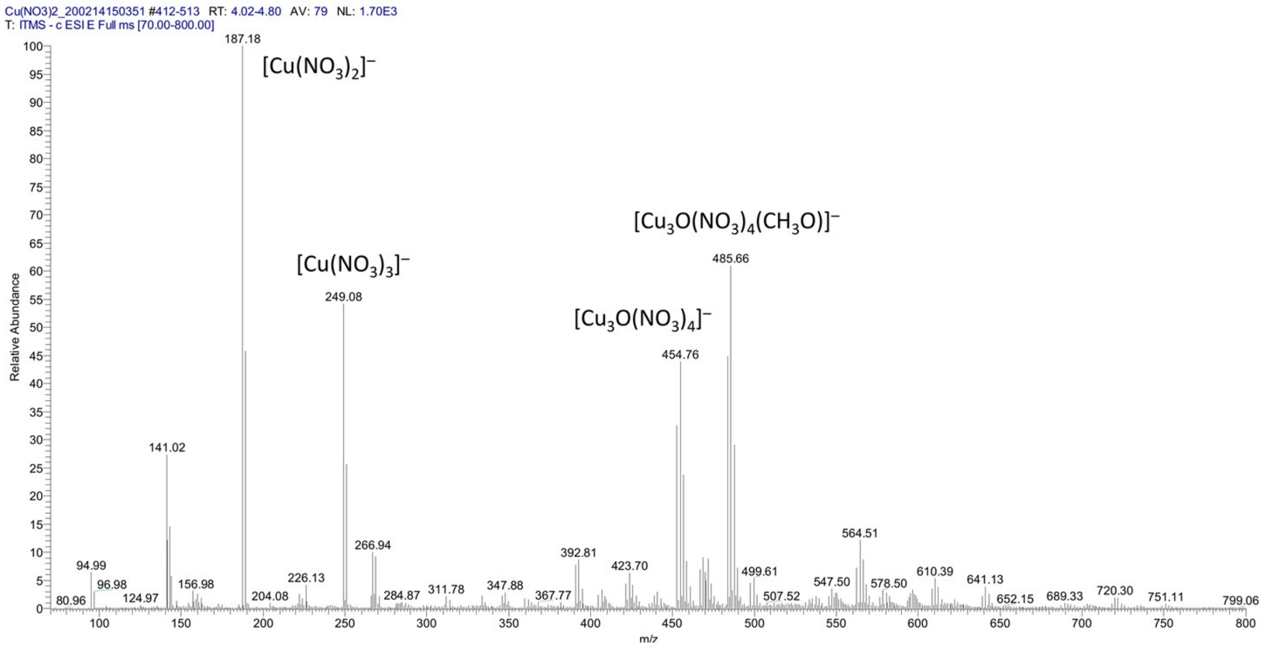

Figure S14. ESI-MS spectra of 1 mM solutions of $CuCl_2 \cdot 2H_2O$ (top) and $Cu(NO_3)_2 \cdot 2H_2O$ (bottom) in methanol.

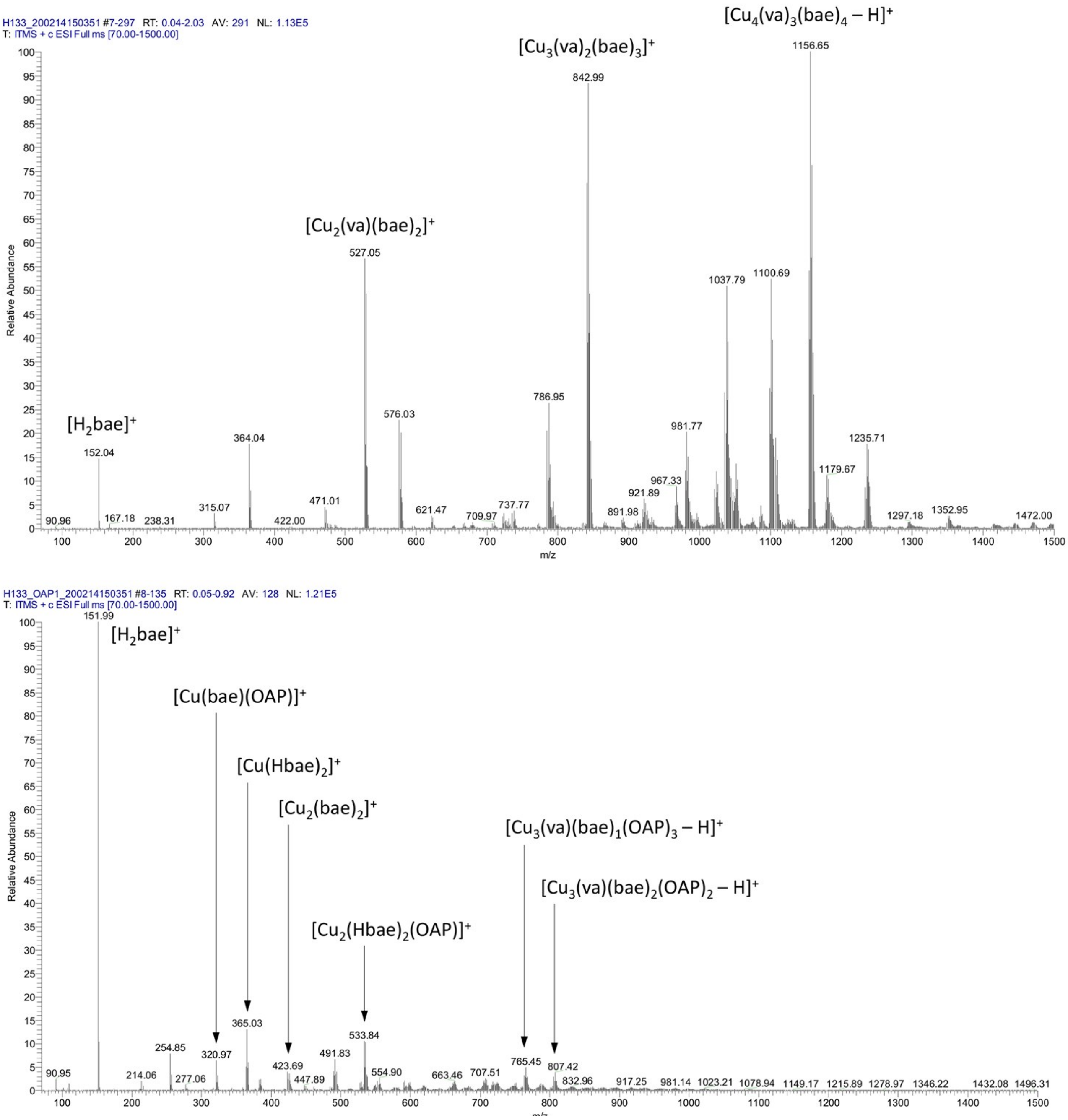

Figure S15. ESI-MS spectra of 1mM of **3** in methanol (top) and of the catalytic mixture of **3** (1 mM) and OAP (10 mM) in methanol taken one minute after the reaction initiation (bottom).

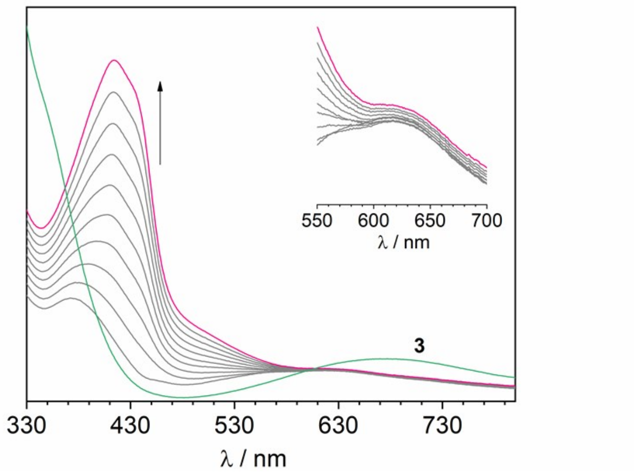

Figure S16. Increase in the phenoxazine band (435 nm) over time (the spectra were recoded with 2 min intervals) in the oxidation of OAP (2.4 mM) catalysed by **3** ($[Cu]_0$ = 0.5 mM) in CH_3OH at room temperature. Green line shows the absorption spectra of pure **3** (1 mM) in CH_3OH taken. Inset shows evolution of 620 nm absorption with time.

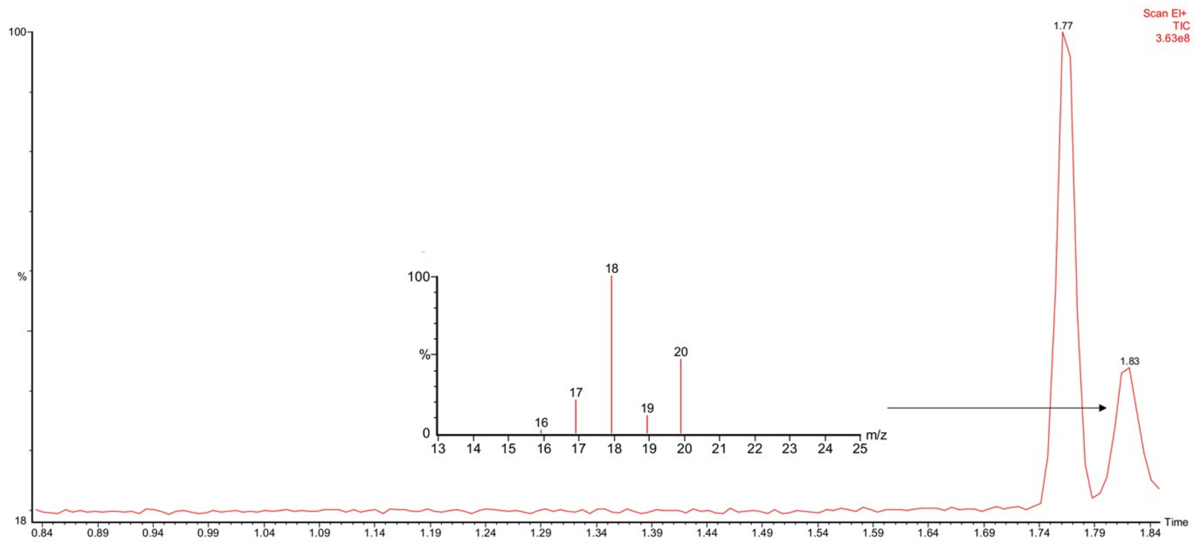

Figure S17. Fragment of the chromatogram, showing the peaks of dioxygen (1.77 min) and water (1.83) in the oxidation of OAP (10 mM) with $^{18}O_2$, catalysed by **3** (1.2 mM), in methanol, after 3 h. The inset shows the EI mass-spectrum that discloses the presence of $H_2{}^{18}O$.

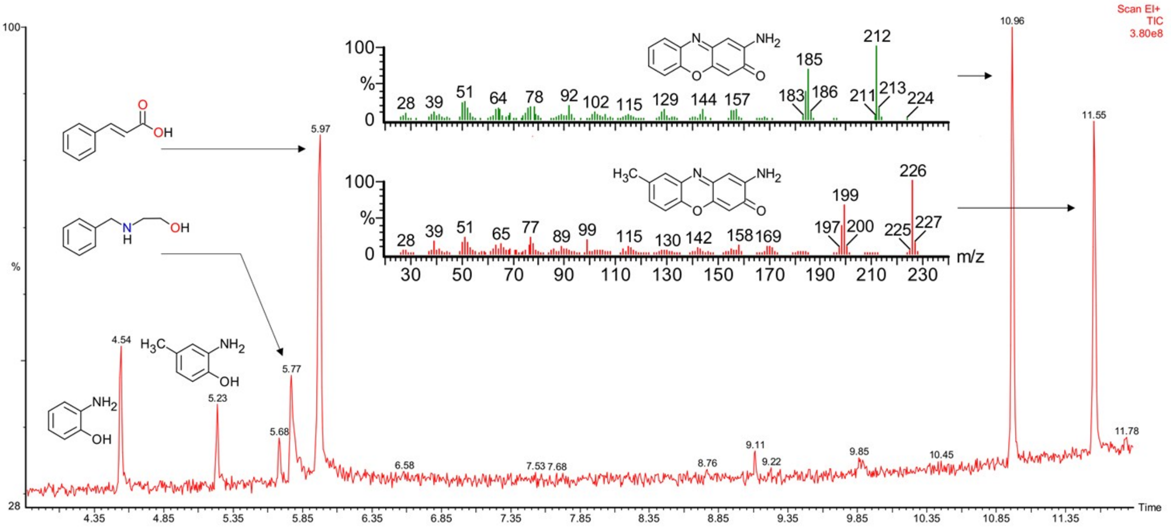

Figure S18. Fragment of the chromatogram showing the reaction products, non-reacted substrates and ligands in the oxidation of oxidation of 2-amino-*p*-cresol (APC) and *o*-aminophenol (OAP), 5 mM each, catalysed by **1** (1 mM). The inset shows the EI mass-spectra of the products.

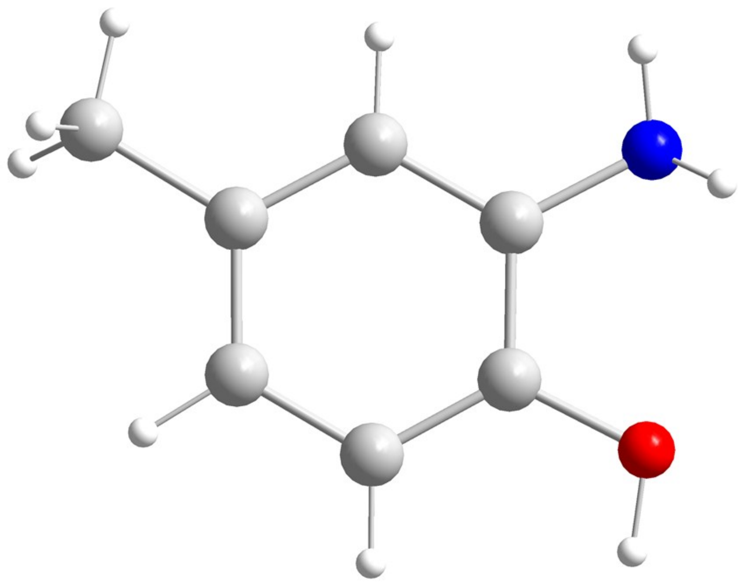

Figure S19. The ball-and-stick representation of the structure of **4**.

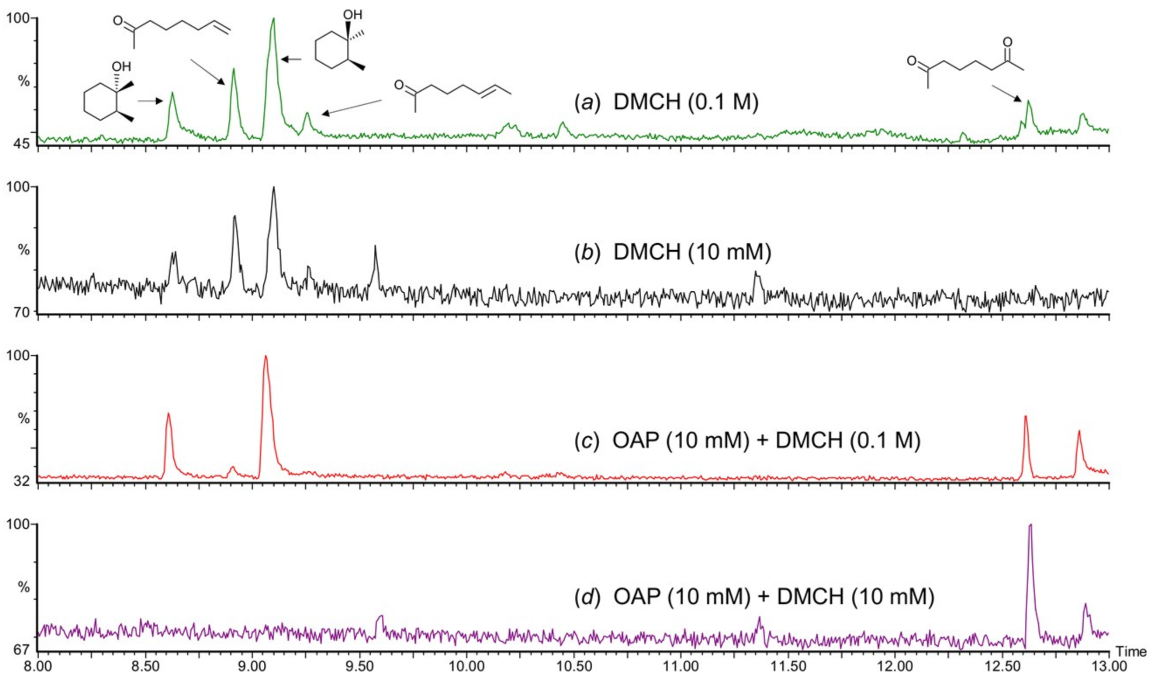

Figure S20. Fragments of the chromatograms showing the products of the aerobic oxidation of *cis*-1,2-dimethylcyclohexane, catalysed by **3** (1.5 mM), in the presence or absence of OAP.